A Channel Model of Atmospheric Impairment for the Design of Adaptive Coding and Modulation in Stratospheric Communication

GORAZD KANDUS*, MIHAEL MOHORČIČ*, MIHA SMOLNIKAR*, ERICH LEITGEB+ and TOMAŽ JAVORNIK*
*Department of Communication systems, +Institute of Broadband Communications
*Jožef Stefan Institute, +Graz University of Technology
*Jamova 39, SI-1000 Ljubljana, +Inffeldgasse 12, 8010 Graz
*SLOVENIA, +AUSTRIA
tomaz.javornik@ijs.si, gorazd.kandus@ijs.si, miha.mohorcic@ijs.si, miha.smolnikar@ijs.si, erich.leitgeb@tugraz.at

Abstract: - Wireless communication in the millimetre frequency bands is subject to severe atmospheric impairment caused by rain and scintillation, which may occasionally cause deep fades and thus needs to be mitigated by an efficient countermeasure such as adaptive coding and modulation (ACM). In this paper we focus on stratospheric communication and propose appropriate rain and scintillation fading channel models, which we use to describe the conceptual design of adaptive coding and modulation on four reference theoretical ACM schemes. Rain fading is modelled according to the modified DLR segment approach for generating channel attenuation time series, taking into consideration the specifics of stratospheric communication systems, namely the variable elevation angle and different carrier frequency. Additional fading due to scintillation, which may be harmful in deep fades caused by the rain, is modelled by adjusting the satellite scintillation channel model so that the amount of scintillation fading is correlated to the attenuation caused by the rain. We describe two extreme approaches to the ACM design process, one for maximizing the system reliability and the other for maximizing the system throughput. We present simulation results for four representative theoretical ACM schemes with different SNR ranges as the variation of bandwidth efficiency in time, and as system outage probability. Finally we show that, for a given SNR range, increasing system complexity by increasing the number of different coding-modulation (CM) modes beyond a certain optimum value does not yield a notable increase in bandwidth efficiency. In other words, there is a trade off between the system complexity and bandwidth efficiency that needs to be taken into account when designing the ACM scheme. Finally, two standards with ACM schemes applicable for stratospheric communications are proposed and analyzed, namely IEEE standard 802.16 for single carrier transmission and ETSI standard for digital video broadcasting over satellites DVB-S2.

Key-Words: - rain fading, scintillation fading, millimetre frequency band, stratospheric communication system, propagation channel model, adaptive coding and modulation

1 Introduction

In millimetre frequency bands atmospheric impairment, such as rain attenuation and scintillation, may cause severe degradation of the system performance, even under line of sight (LOS) channel conditions [1,2]. Additional channel loss due to heavy rain may exceed 10 dB or even 20 dB, and may cause system outage, unless efficient countermeasures are taken. In reality, atmospheric impairment is slow compared to the frame rate, thus a close loop adaptation of the system parameters is feasible. A straightforward increase of the transmit power is not a practical solution due to limited power resources at the base and subscriber stations, possible increase of co-channel interference, the design of high power amplifiers, safety reasons, etc. A promising solution, also foreseen in the latest wireless communications standards, is based on adjusting the coding and modulation scheme according to the state of the current propagation channel [3,4,5,6,7,8]. The millimetre frequency bands are predominately allocated for communication systems where LOS channel conditions are expected during system operation, i.e. satellite and stratospheric communications. While atmospheric impairments for satellite communications have

been thoroughly studied, modelling of the stratospheric channel is relatively unexplored.

Stratospheric platforms equipped with a suitable communications payload have recently emerged as a communications infrastructure complementary to currently available terrestrial or satellite wireless communication systems [9,10,11,12]. They can take a form of an airship or airplane, and can be manned or unmanned. These options importantly influence the main parameters of the mission, including the duration, altitude, service scenario, and others. Aerial platforms operating in the lower stratosphere, typically at altitudes between 17 and 22 km, are particularly interesting for the provision of communication services and are usually referred to in the literature as High Altitude Platforms (HAPs) [13]. There are numerous advantages of stratospheric over satellite communication systems. These include easy and low cost launching of the platform, low propagation delay, smaller size of terminal equipment, lower power consumption and the possibility of landing the platform for maintenance, replacement and upgrading of the equipment. Compared to terrestrial broadband wireless access systems, which are characterized by a harsh multi-path propagation environment, the propagation channel to and from a stratospheric platform can most of the time be considered as line of sight (LOS) due to the high elevation angle between the user and HAP, which results in less complex terminals achieving higher data throughput. This is particularly true for fixed point-to-point and point-to-multipoint systems with highly directional antennas.

Depending on the communication services foreseen for the provision via HAPs, the International Telecommunications Union (ITU) permitted the use of several frequency bands, including a band at 2 GHz for 3G mobile communication services [14] and two bands for broadband services in the millimetre-wave frequencies, namely at 47-48 GHz and 28-31 GHz. In order to design, verify and optimize a communication system, a suitable model of the communication channel is required that adequately captures the propagation effects at those frequency bands. The deterministic channel models applying basic principles of radio wave propagation, such as reflection, diffraction, scattering, etc., are too complex and, additionally, require huge databases on the operating environment, with the geometrical and electrical characteristics of obstacles. The empirical channel models thus provide a good compromise between accuracy and complexity. However, good channel models are typically based on measurement campaigns carried out over long periods of time. In the case of the emerging systems, such as one based on stratospheric communications, measurement campaigns are not possible, due to non-existent equipment, i.e. a stable flying stratospheric platform equipped with communication payload. In this paper we propose to solve the problem by taking an existing, though similar, channel model and modifying its parameters according to the specifics of the analyzed communication system. Thus, we have adapted models of rain attenuation and scintillation of the satellite channels at the millimetre frequency band in order to model the stratospheric communication channel. This model is then used to describe a conceptual approach to designing adaptive coding and modulation optimized to spectral efficiency.

This paper is organized as follows. First, the differences between satellite propagation and stratospheric propagation channels are summarized in Section 2. A new channel model of rain attenuation and scintillation for stratospheric communications is proposed and described in Sections 3 and 4. The simulation tool for generating a channel attenuation time series is described in Section 5. This is followed in Section 6 by an example of the adaptive coding and modulation design to combat rain fading in stratospheric communication systems. Finally, in Section 7, we discuss some representative results and conclude with further ideas to improve the model and its application.

2 Comparison of satellite and stratospheric propagation channels

The LOS propagation conditions between transmitter and receiver and the similar elevation angles are the two most important common characteristics of satellite and stratospheric propagation channels [15,16]. These characteristics allow satellite channel models to be used as a baseline for designing stratospheric channel models. However, there are two important distinctions between stratospheric and satellite communication systems that have to be taken into account when modelling the stratospheric channel:

- The distance between the receiver and transmitter is significantly shorter in the case of stratospheric systems.

- The rate of and reason for elevation angle variation are different. In the case of GEO satellites, the elevation angle does not vary significantly when the mobile terminal changes its position. In LEO satellite systems the rate of variation of the elevation angle is comparable to that in stratospheric systems, but is caused mainly by satellite motion and, for that reason, is easily predictable.

Due to these differences the satellite channel models are not directly applicable for describing propagation conditions in stratospheric communications and some modifications are required.

Fluctuation of the amplitude and phase of the received signal due to rain and scintillation are among the major problems in the design of satellite and stratospheric communication links operating in the millimetre frequency bands. In the following sections we describe both phenomena and the approach to their modelling in stratospheric communications.

3 Rain attenuation

Rain fading is a form of signal attenuation caused by precipitation, clouds and other meteorological phenomena, where precipitations have the most significant influence. It causes sporadic signal attenuation in satellite and terrestrial communication systems operating on millimetre frequency bands. The impact of rain fading on communication system performance depends mainly on the rain rate, type of the rain (showers, heavy rain, drizzle, etc.) and the thickness of clouds. Rain fading is typically characterized by the corresponding climate zone as defined by ITU-R. The ITU-R provides recommendations concerning the effects of rain on radio wave propagation, but the recommendations refer to average conditions, which are not sufficient for the process of design and analysis of the communication systems. Thus, typical approaches for modelling rain attenuation are based either on converting meteorological data into channel attenuation time series or on setting the parameters of a time series attenuation generator according to the measurement results obtained by long term measurement campaigns [17].

In satellite communication systems, two basic approaches that constitute a good compromise between channel model accuracy and complexity have been used to model rain fading and to generate the time series of attenuation:

- The Markov chain approach used in the ONERA simulator [17,18] and
- The DLR segment approach [17,19].

The ONERA Markov channel model [18] consists of macroscopic and microscopic models, with a component that combines the outputs of each. The macroscopic model is a 2-state Markov chain consisting of rain state and clear sky state. It follows the long-term behaviour of rain fading, taking into account the mean duration of rain events. The parameters of macroscopic models can be derived from the radio meteorological data banks such as ITU-R or the European Centre for Medium-Range Weather Forecasts (ECMWF) [20]. The ITU-R P.387 Recommendation provides the probability of rain averaged over one year, from which all necessary macroscopic parameters of the model can be calculated. The microscopic model is an N-state Markov chain which generates the time series with high resolution and gives the short-term dynamic behaviour of rain attenuation [17].

The DLR segment channel approach is based on a Markov chain and a Gaussian random variables generator [17,19]. It consists of a generic part together with a specific set of parameters that allow adjustment of the channel model to different elevation angles, carrier frequencies and climatic zones. The model specifies three types of channel attenuation segment:

- The channel attenuation segment with almost constant received power, referred to as *C-segment*.
- The channel attenuation segment with mainly monotonously decreasing channel attenuation, referred to as *D-segment*.
- The channel attenuation segment with mainly monotonously increasing channel attenuation, referred to as *U-segment*.

For each segment the conditional distribution $P(y|x)$ is calculated based on a measurement campaign. The conditional distribution $P(y|x)$ denotes the likelihood that the current channel attenuation in dB is y conditioned that $\Delta\tau$ seconds before the attenuation has been x. Satellite channel measurements show that $\Delta\tau$ is around 1s and that $P(y|x)$ obeys a Gaussian distribution. The standard deviation and mean value of the Gaussian distribution depend on the segment (C,U,D), the current attenuation and on location (latitude, longitude) of measurements and satellite elevation angle. Switching between attenuation segments of the channel is determined by calculating the difference between channel attenuation in

successive time intervals i.e. $\Delta a(iT)=a(iT)-a((i-1)T)$, where $a(iT)$ denotes the attenuation at i-th time (interval)

$$\Delta a(iT)=\begin{cases}|a(iT)-a((i-1)T)| & <1dB, \quad \text{C segment}\\ a(iT)-a((i-1)T) & \geq 1dB, \quad \text{D segment}\\ a(iT)-a((i-1)T) & \leq 1dB, \quad \text{U segment}\end{cases}. \quad (1)$$

The algorithm of the DLR segment model can be summarized in the following three steps [17]:

1. Calculate the attenuation segment type from $a(iT)$, $a((i-1)T)$.
2. Obtain the mean value and standard deviation from the lookup table, taking into account attenuation segment type and current attenuation $a(iT)$.
3. Generate the attenuation for the next time interval $a((i+1)T)$.

A rain fading event with the C, D and U segment is illustrated in Fig. 1. The lookup tables [17] for mean value and standard deviation of the Gaussian process are calculated by processing measurements obtained from the measurement campaign at DLR Obrepfaffenhofen (11.3° East, 48.1° North) with the satellite elevation angle equal to 34.8°, the ITU-R climate zone K and the carrier frequency 40 GHz. The analysis shows that the standard deviation and mean value depend significantly on the season of the year.

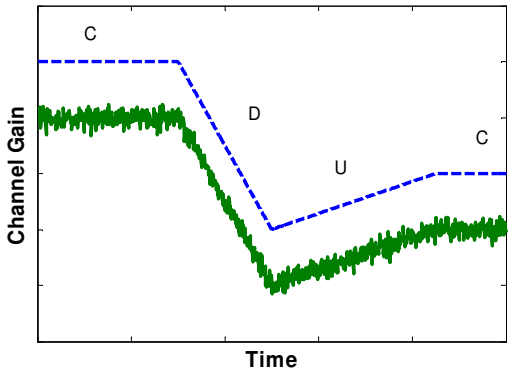

Fig. 1. DLR segment approach for rain fading

For rain attenuation in stratospheric communication systems we used the DLR segment model based on the measurement campaign described above. However, since the carrier frequency and the elevation angles for HAP-based communication systems are significantly different from those used in the measurement campaign [17,19], resulting in a different path length affected by rain, we adjusted the DLR segment model by introducing the frequency correction term and normalizing the rain attenuation on a per kilometre basis.

The model proposed by CCIR Report 721-1 [21] and accepted by ITU-R P Series [22] was applied to correct the attenuation due to different carrier frequencies

$$\frac{A_1}{A_2}=\frac{g(f_1)}{g(f_2)}, \quad (2)$$

where A_1 and A_2 are attenuations at frequencies f_1 and f_2, and $g(f)$ is defined by

$$g(f)=\frac{f^{1.72}}{1+3\cdot 10^{-7}\left(f^{1.72}\right)^2}, \quad (3)$$

where f is the frequency in GHz.

The results published in [17], were obtained for fixed elevation angle, and consequently for fixed length of radio ray affected by the rain. HAP, on the other hand, can be seen at different elevation angles due to the motion round the nominal position, thus the path affected by rain is different. In order to capture this effect we normalized to 1 km the results obtained from the DLR sequence model using ITU-R recommendation PN 618-4 [23] for slant path length calculation, according to the following procedure:

1. Calculate the effective rain height h_R:

$$h_R[km]=\begin{cases}3.0+0.028\phi & 0^\circ \leq \phi < 36^\circ\\ 4.0-0.075(\phi-36) & 36^\circ \leq \phi\end{cases}, \quad (4)$$

where ϕ is the latitude of the Earth station.

2. Calculate the slant path length L_S[km] below the rain height:

$$L_S[km]=\begin{cases}\dfrac{h_R-h_S}{\sin\theta} & \theta \leq 5^\circ\\ \dfrac{2(h_R-h_S)}{\left(\sin^2\theta+\dfrac{2(h_R-h_S)}{R_e}\right)^{1/2}+\sin\theta} & \theta > 5^\circ\end{cases}, \quad (5)$$

where θ is the elevation angle, h_S[km] is the Earth station's altitude above sea level and R_e is the equivalent radius of the Earth.

3. Multiply the distance from HAP in km by the normalized attenuation to obtain the rain attenuation in dB.

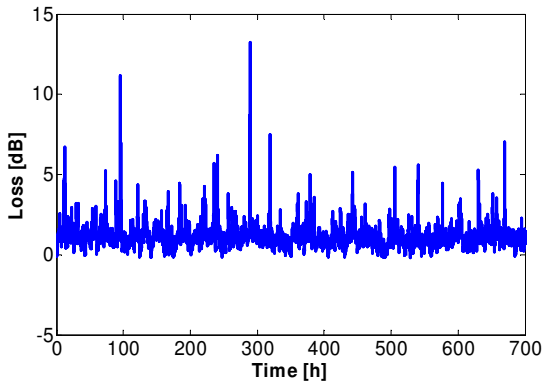

Fig. 2. Rain attenuation time series generated for HAP operating environment

An example of rain attenuation time series is illustrated in Fig. 2, calculated for approximately 30 days in spring and for a fixed stratospheric communication system. Sporadic rain events can be observed causing attenuation from a few dB to almost 15 dB. Such rain attenuation typically results in degradation of system performance, so it needs to be compensated by suitable fade mitigation techniques. The dynamic range of channel variation shown in this example, i.e. 15 dB (Fig. 2), can easily be treated with the adaptive coding and modulation approach proposed for instance in DVB-S2 standard [24], assuming slow channel variation.

4 Scintillation

Scintillation refers to the rapid fluctuation in signal amplitude and phase [25,26,27]. The effects are often observed in satellite links and may occur either in the ionosphere, due to changes in free electron density, and/or in the atmosphere, due to changes in pressure, humidity, temperature, etc. HAPs fly below the ionosphere, so we are interested only in scintillation caused in the atmosphere, where tropospheric scintillation dominates [28].

The main causes of tropospheric scintillation are moisture content and its turbulent mixing in the atmosphere. Rain, clouds, wind, multipath propagation, size of antenna and wavelength affect scintillation characteristics. In general, scintillation increases with decreasing antenna, increasing temperature and moisture content, decreasing elevation angle and higher carrier frequency. Fading, including tropospheric scintillation, is usually described using the log-amplitude and log-amplitude variance of the signal [27]. Many models of the expected statistics for log-amplitude and log-amplitude variance have been proposed. The majority model short term log-amplitude scintillation as a Gaussian probability density function with standard deviation σ.

The scintillation may become a relevant source of errors in a communication system operating at low elevation angles with antennas with small apertures. Fortunately, this is not the case in stratospheric communication systems, where the elevation angle is never below 5° and the antenna apertures are rather large. However, in the case of rain attenuation, the scintillation may decrease the availability of the system, so we are particularly interested in scintillation models that describe the correlation of scintillation with rain attenuation.

It was found [26] that the conditional average standard deviation of tropospheric scintillation is linked to attenuation by the power law. It can be predicted by a very simple physical model, such as a turbulent thin layer aloft during the rain event, that indicates an increase of tropospheric scintillation during rain. The correlation between the rain attenuation and the scintillation is summarized in the following equation [26]

$$\sigma = \begin{cases} \sigma_0 \ [\mathrm{dB}] & \text{if } A < 1\,\mathrm{dB} \\ \sigma_0 \cdot A^{5/12} \ [\mathrm{dB}] & \text{if } A > 1\,\mathrm{dB} \end{cases}, \quad (6)$$

where σ_0 is the standard deviation of scintillation before the rain event, σ is the standard deviation of the scintillation and A the attenuation due to the rain event. The correlation between the rain attenuation and scintillation does not provide any knowledge about the spectral properties of the scintillation. This is given in [27] where Tatarskii's theory [29] on propagation through a turbulent media is applied to obtain the spectrum of scintillation in clear sky.

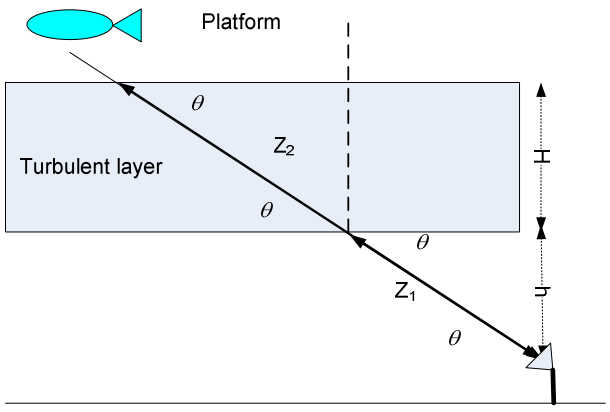

Fig. 3. Geometry of the scintillation model for the HAP operating environment

According to the theory, the power spectrum density of scintillation in clear sky is flat for frequencies lower than the corner frequency f_c, and it has a slope of –80 dB/dec at higher frequencies, all in log-log scale of the graph. The corner frequency can be deduced either from the theoretical model [29] or estimated from measurement campaigns [26]. With certain assumptions, the theoretical value of the corner frequency can be calculated as

$$f_c = 1.425 f_0 \left(\frac{1 - \frac{z_1}{z_2}}{1 - \left(\frac{z_1}{z_2}\right)^{11/6}} \right)^{3/8}, \quad (7)$$

where $f_0 = \frac{1}{2\pi} V_t \sqrt{\frac{k}{z}}$, V_t is the transverse velocity of the wind, k is the wave number, $L = z_2 - z_1 = H/\sin\theta$ is the thickness of the turbulent layer extending from z_1 to z_2 along the path, $z = 0.5\,(z_1 + z_2)$, H is the mean turbulent layer height and θ is the path elevation angle. Typical values for the corner frequency lie between 0.1 Hz and 0.6 Hz. The geometry of the model is shown in Fig. 3.

As in satellite links, the signal fading due to scintillation in stratospheric links depends on the length of the path through the turbulent layer. As shown in Fig. 3 the length of the path through the turbulent layer depends strongly on the elevation angle. Consequently, the results obtained for scintillation from the satellite model are not directly applicable to stratospheric communications, for the same reason as in the case of rain attenuation. So we propose a procedure, similar to that for the rain attenuation, to introduce the elevation angle dependency into the expression for the corner frequency. According to Fig. 3, we express the path lengths z_1 and z_2 as functions of the mean turbulent layer height H, elevation angle θ and the altitude of the turbulent layer h

$$z_1 = \frac{h}{\sin\theta} \qquad z_2 = \frac{H+h}{\sin\theta}. \quad (8)$$

By inserting (8) in (7), the corner frequency can be expressed as

$$f_c(\theta) = \frac{1.425}{2\pi} V_t \sqrt{k \frac{2\sin\theta}{2h+H}} \left(\frac{1 - \frac{h}{H+h}}{1 - \left(\frac{h}{H+h}\right)^{11/6}} \right)^{3/8}. \quad (9)$$

Assuming the corner frequency $f_c(\theta_0)$ is known for an elevation angle θ_0, the calculation of the corner frequency for an arbitrary elevation angle is straightforward

$$f_c(\theta) = \sqrt{\frac{\sin\theta}{\sin\theta_0}} f_c(\theta_0). \quad (10)$$

In our simulations we used median values of σ_0, elevation angle θ_0 and corner frequency $f_c(\theta_0)$, which were obtained from measurements during the Intelsat experiment in 1994 [26], namely $\theta_0 = 37.8°$, $f_c(\theta_0) = 0.45$ Hz and $\sigma_0 = 0.099$.

Two examples of fading due to scintillation are illustrated in Fig. 4 for an elevation angle of 38°. The lower trace represents the scintillation in the channel without rain (rain attenuation equal to 0dB) with the range of amplitude variation equal to approximately 0.01dB, while the upper trace stands for shifted scintillation loss for rain attenuation of 20dB. In the latter case the variation of amplitude range is in the range of approximately 0.3dB.

According to the proposed model, the standard deviation of the scintillation is greater for greater rain attenuation, as is clearly seen from the generated time series of scintillation fading. Since the elevation angles are the same in each case, the corner frequency is the same for both examples. At low elevation angles the path through the turbulent layer is longer, resulting in higher attenuation due to rain and lower corner frequency, with the consequence of slower variation of fading due to scintillation.

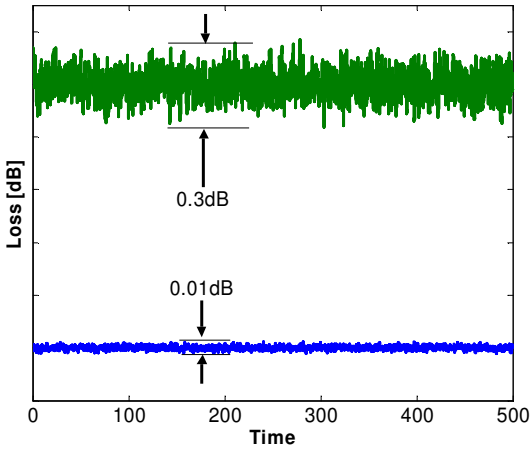

Fig. 4. Attenuation time series due to the scintillation effect generated for HAP operating environment

5 HAP channel simulator

The proposed models were built into a software tool for generating attenuation time series for stratospheric communications, either mobile or fixed. The channel simulator is able to generate the

attenuation time series for the following propagation phenomena:

- free space loss attenuation,
- rain fading [see Section 3],
- scintillation [see Section 4] and
- a mobile HAP channel considering the attenuation due to shadowing and blocking [15].

Fig. 5 shows the graphical user interface of the simulator, which enables the appropriate channel model to be chosen, and enters the parameters for selected channel models. The graphical user interface is divided into the following sections:

- the GIS data section enables the file containing the digital elevation model of terrain, and the clutter file defining the coverage of terrain by vegetation, for example wood and the path of vehicle through area, to be entered,
- the HAP section with inputs about the HAP position and antenna type,
- the parameters & run simulation section, with selection of the channel model and inputs of the most important channel parameters, and finally,
- combined simulations from the file section whose main purpose is to combine and compare simulations with different parameters.

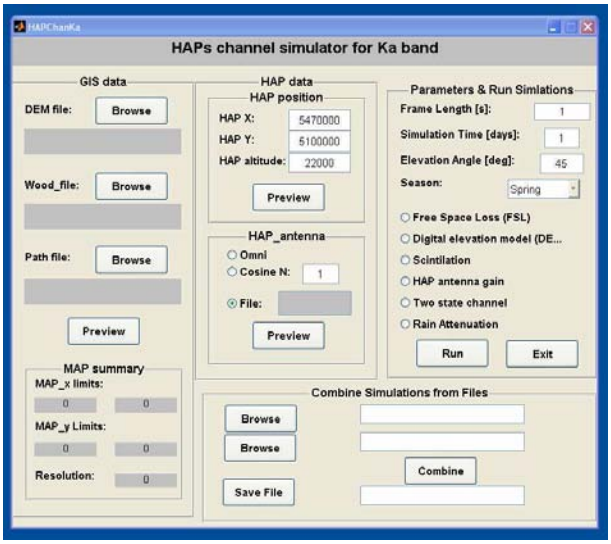

Fig. 5. Graphical user interface of the HAP channel simulator

The channel simulator depicted in Fig. 5 has been applied for generating the attenuation time series in this paper.

6 Design of the adaptive coding modulation scheme for mitigating rain fading

As mentioned previously, adaptive coding and modulation is a powerful means of mitigating the impairment due to rain fading [3,4,5,6,7,8,24,30,31]. The typical simulation model of a telecommunication system with ACM scheme is depicted in Fig. 6. It consists of four parts, namely

- the transmitter part,
- the receiver part,
- the propagation (forward) channel and
- the return channel.

The pilot and synchronization symbols, applied for fast channel estimation and synchronization at the receiver, are added to information symbols at the transmitter. In the next block the information bits are encoded taking into account the estimated channel conditions and available set of coding-modulation (CM) modes, and then transformed into signal waveforms that are transmitted over the propagation channel. The propagation channel distorts the transmitted waveforms. At the receiver, the channel conditions are estimated in the channel estimator and, in the mod-cod mode selector block, the most appropriate CM mode for the next transmission frame is then determined. The estimated channel conditions may also help in demodulating and decoding the information bits. The data concerning the selected CM mode are transmitted to the receiver via the return channel back to the transmitter. Typically the return channel is assumed to be ideal, i.e. error free, in the majority of ACM scheme analyses.

The most important task of the ACM design is to determine the set of CM modes and the switching criteria for selecting the CM mode transmitted under the light of channel conditions. The number of CM modes in ACM schemes depends strongly on the transmission channel characteristics, i.e. its SNR variation range, speed of variation, required data rate, propagation channel selectivity, channel bandwidth, etc. In this section we will analyse the impact of the ACM scheme parameters, i.e. the SNR range covered by the CM modes and the number of CM modes on the system performance.

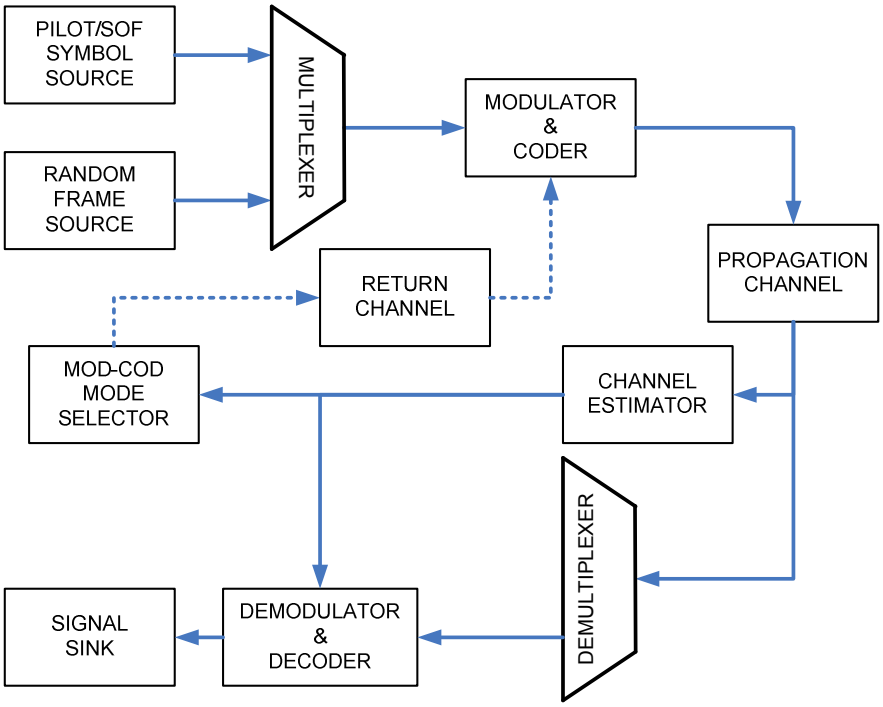

Fig. 6. Block diagram of communication system with adaptive coding and modulation (ACM)

Analysis of the channel loss in Fig. 2 indicates that, in time intervals during which the communication link is not affected by heavy rain, the channel loss varies between 0 dB and 2 dB, and that the heavy rain occasionally causes deep fades, in some cases higher than 10 dB. For complete mitigation of such deep fades the ACM scheme should consist of CM modes, with their operating signal-to-noise (SNR) range covering the expected maximum variation of the channel loss. However, in operating communication systems we are typically limited to a finite set of CM modes covering only a part of the required SNR range, so complete mitigation of rain fading is not possible. For that reason, the maximum probability of system outage or expected number of hours per year with the received signal below receiver sensitivity is given in satellite communication systems.

Assuming an ACM scheme that cannot cover the whole range of channel gains with its limited number of CM modes, the link budget can be designed either to maximize the system reliability or to maximize the system throughput. In the former approach for maximizing system reliability, the system is designed so as to guarantee reliable communications with the required bit error rate (BER) level, even under the worst expected channel conditions. This means that the most robust (the most power efficient) CM mode is applied in the worst channel state and more bandwidth efficient CM modes are used in less harmful channels. The application of such an approach results in a certain loss of system throughput. In the approach to maximize system throughput, the link budget is designed to provide the highest possible throughput by applying the most bandwidth efficient CM mode under the best channel conditions. Less bandwidth efficient modes are applied for worse channel conditions to partially compensate for fading. When the received SNR is lower than the SNR threshold of the most power efficient CM mode, the system becomes unavailable. This approach may result in increased system outage. The trade off between the probability of system outage and system throughput can be achieved by combining the two approaches.

Considering the channel losses in Fig. 2 we applied a heuristic approach to design the link budget for time intervals without heavy rain. In particular, the transmit power and switching thresholds have to be determined in the design procedure. The design procedure goes as follows. First we calculate the switching thresholds from the performance curves of CM modes represented by BER as a function of SNR. An example of BER curves is shown in Fig. 7. Let us assume that the service provided by a telecommunication system requires a BER lower than 10^{-3}. In order to provide higher layers of the protocol stack with BER below the target value, the threshold for switching

between two CM modes is obtained by drawing a horizontal line at the target BER. The line intersects the BER curves. The projections of the intersection points on the abscissa define the thresholds for switching between CM modes. The most robust CM mode is used when the SNR lies between the projection of the first (Th1) and second intersection points (Th2). The information is carried by the second CM mode, when SNR is between the second (Th2) and the third projection of intersection points (Th3). The CM mode with the highest spectral efficiency is applied for SNR higher than the projection of the last intersection point (Th3) on the abscissa. When the SNR ratio is lower than the first intersection point (Th1), the target BER cannot be achieved and no information is transmitted. The BER curves may be generated by computer simulations or even obtained by measuring the implemented communication systems.

In order to guarantee the required SNR at the detection of the received signal, the transmit power of the signal has to be estimated, taking into account channel loss, noise floor and required SNR

$$SNR[\mathrm{dB}] = P_t[\mathrm{dBW}] - L[\mathrm{dB}] - N_{floor}[\mathrm{dBW}], \quad (11)$$

where P_t is transmit power in dBW, L is channel loss in dB, and N_{floor} denotes noise floor in dBW. The noise floor depends on system bandwidth, noise temperature, realization of the receiver, noise figures of low noise amplifiers used at the receiver, etc., and can easily be estimated knowing the details of the receiver design. Next, the channel loss is calculated for clear sky conditions. 1 dB is added to the calculated clear sky channel loss to ensure the use of the most bandwidth efficient CM mode in non perfect clear sky conditions. The transmit power P_t can be calculated by applying equation (11). To estimate the theoretical ACM scheme performance, the thresholds for other CM modes are determined according to the SNR range and number of CM modes in the ACM scheme, assuming equal SNR distance between CM modes at target BER. For a system with a predefined set of CM modes, the SNR distances between neighbouring CM modes are not constant, so switching thresholds are determined according to the intersection of BER curves with the horizontal line determining target BER rate as depicted in Fig. 7.

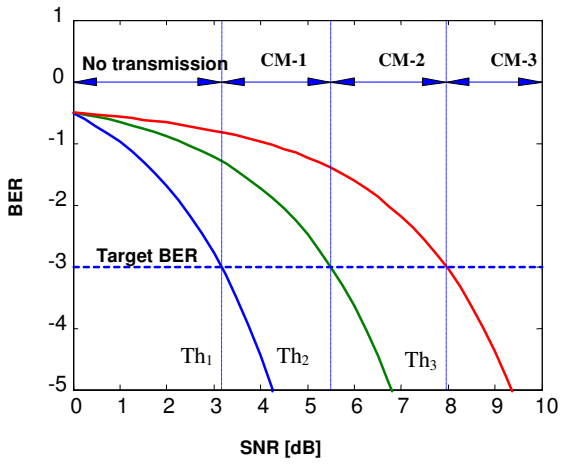

Fig. 7. Design of ACM thresholds for the maximum throughput criteria

In order to test the applicability of the generated time series of atmospheric impairments we applied the previously described approach of an ACM scheme designed on a set of reference theoretical (fictitious) ACM schemes with different SNR ranges and different numbers of CM modes in the ACM scheme. The main parameters of the ACM schemes are listed in Table 1.

The SNR ranges and bandwidth efficiencies are chosen to match the SNR range and bandwidth efficiency of DVB-S [32] and DVB-S2 [24] standards, selecting either the entire range of CM modes or only a subset, e.g. only CM modes with QPSK modulation in DVB-S2 standard. The number of CM modes in a given ACM scheme varies between 1 and 30. Other CM modes are spread equidistantly on the line connecting the most bandwidth efficient and the most power efficient CM modes on the bandwidth efficiency/SNR plane.

Time variations of the bandwidth efficiency for the reference ACM schemes with different SNR range are given in Fig. 8 to Fig. 11, assuming the channel loss depicted in Fig. 2. In the case of a SNR range of 18 dB (Fig. 8), the reliability of the communication link is guaranteed for deep fades, while using the most bandwidth efficient CM modes for good channel conditions. The two most robust CM modes are not used at all. In the case where the channel loss represents the heavy rain part of the year, the SNR range of the ACM may be overestimated and a smaller range might yield similar results with much lower system complexity.

While the ACM scheme with an SNR range of 9 dB still provides acceptable system performance, with a negligible system outage time of 0.018%, the ACM scheme with an SNR range of 4.5 dB is not acceptable. As shown in Fig. 11, deep fades cause system outage of approximately 0.29% of time, represented by a bandwidth efficiency equal to zero in Fig. 11. The chosen SNR range is underestimated and an increase is required to provide reliable communication in the heavy rain periods.

ACM scheme	SNR range	Bandwidth Efficiency	SNR range similar to
ACM 1	18.0 dB	0.5 - 4.5	DVB-S2 (all CM modes)
ACM 2	13.5 dB	0.5 - 3.5	DVB-S2 (CM modes based on QPSK-8PSK modulations)
ACM 3	9.0 dB	0.5 - 2.5	DVB-S2 (CM modes based on QPSK modulation)
ACM 4	4.5 dB	0.5 - 1.5	DVB-S

Table 1: Parameters of the ACM schemes

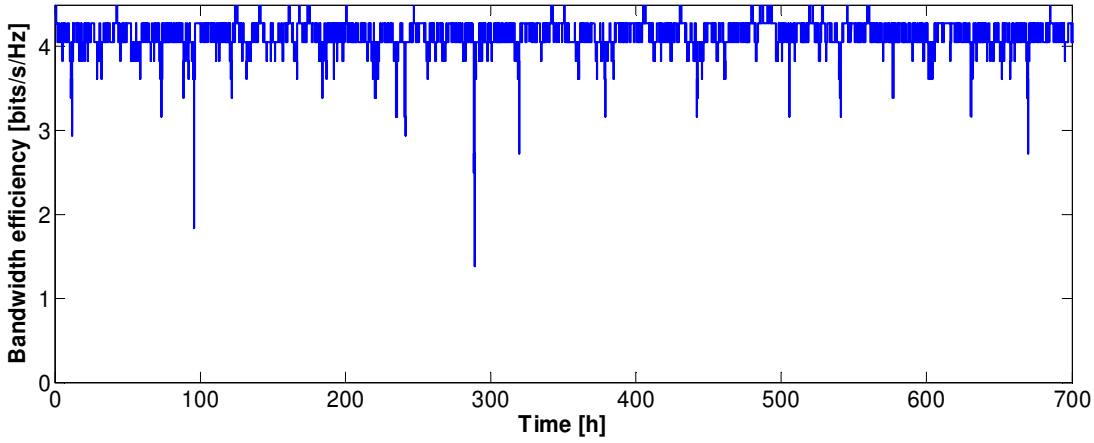

Fig. 8. Time variation of bandwidth efficiency of the scheme ACM 1 with SNR range 18 dB and 18 CM modes

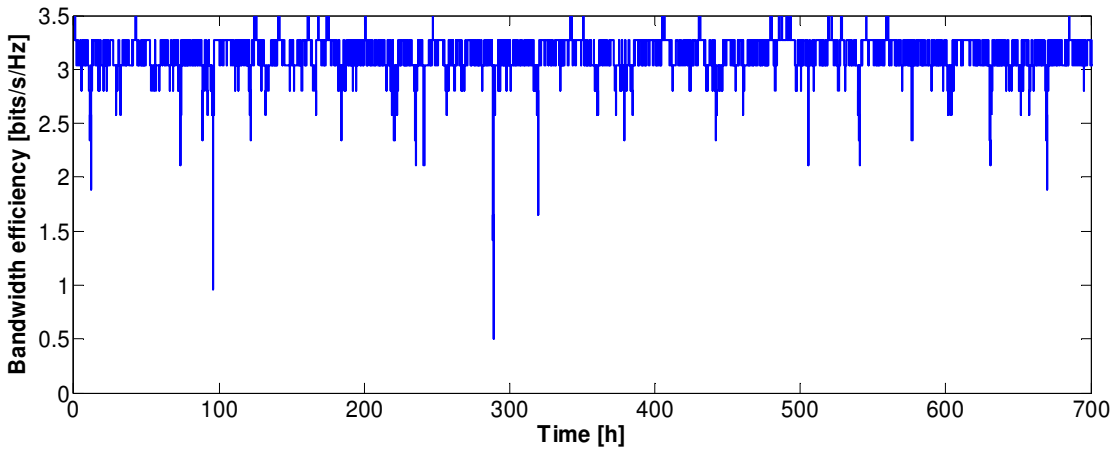

Fig. 9. Time variation of bandwidth efficiency of the scheme ACM 2 with SNR range 13.5 dB and 13 CM modes

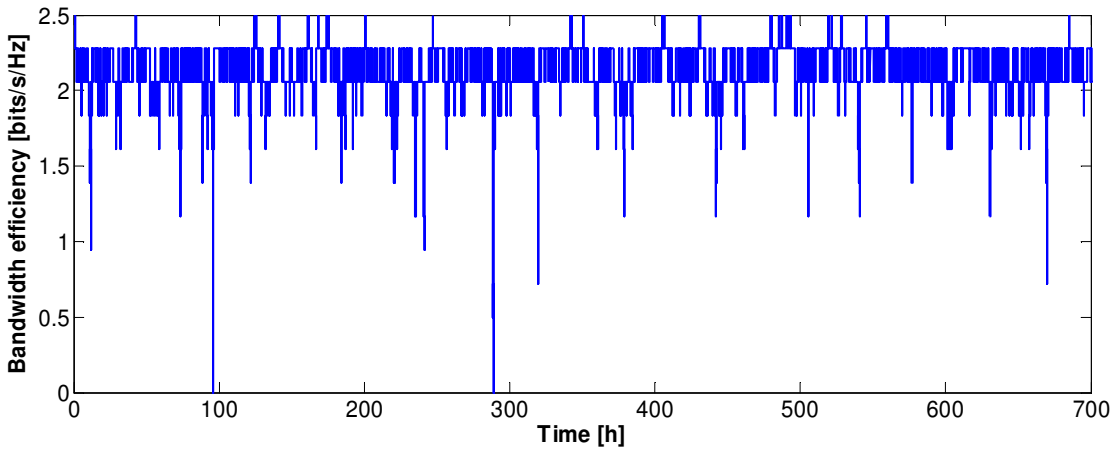

Fig. 10. Time variation of bandwidth efficiency of the scheme ACM 3 with SNR range 9 dB and 9 CM

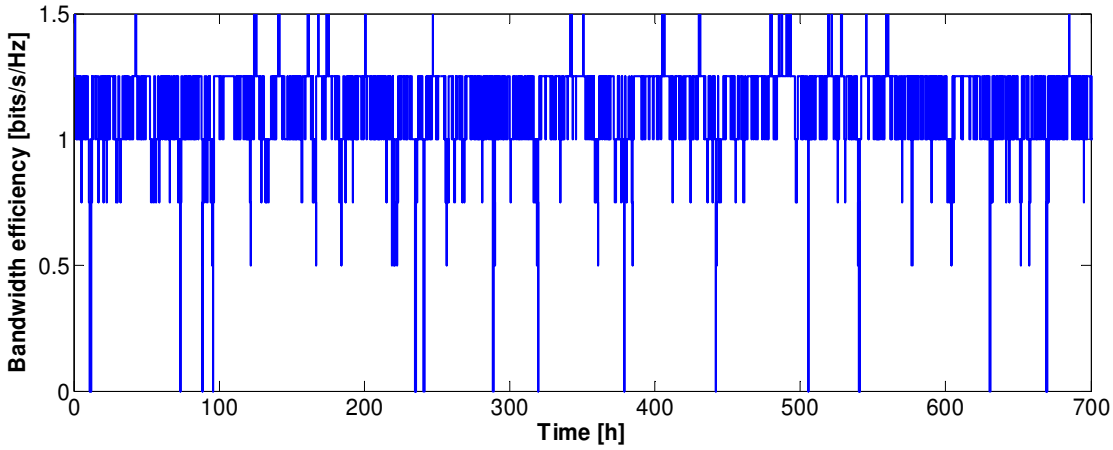

Fig. 11. Time variation of bandwidth efficiency of the scheme ACM 4 with SNR range 4.5 dB and 4 CM modes

The system outage probability of a one month period of rain fading depicted in Fig. 2 is calculated for representative ACM schemes and listed in Table 2.

ACM scheme	SNR range	System Outage Probability
ACM 1	18 dB	0
ACM 2	13.5 dB	0
ACM 3	9.0 dB	$1.8\ 10^{-4}$
ACM 4	4.5 dB	$2.9\ 10^{-3}$

Table 2: System outage for channel loss shown in Fig. 2

Next the optimum number of CM modes in the SNR range should be found. In theory the infinite number of CM modes would give the highest bandwidth efficiency, however in practice an upper limit exists, above which an increase in the number of CM modes does not contribute significantly to the average bandwidth efficiency. A plot of average bandwidth efficiency versus the number of CM modes and SNR range of the ACM scheme is depicted in Fig. 12. As expected, the ACM schemes with larger SNR range provide higher average bandwidth efficiency, however increasing the SNR range beyond the expected channel loss variation does not bring any benefit in terms of average bandwidth efficiency. At low numbers of CM modes, addition of a new CM mode significantly increases the average system bandwidth efficiency, while at higher numbers of CM modes no significant increase of the average bandwidth efficiency is observed.

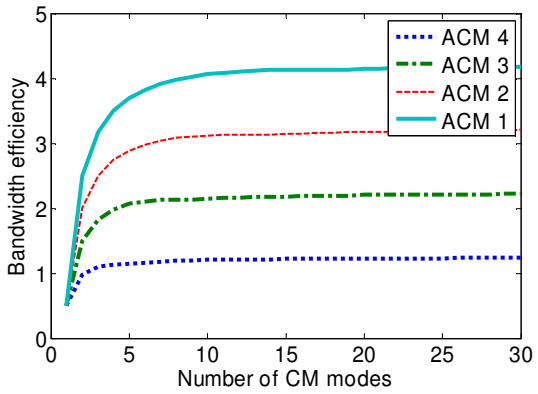

Fig. 12. The average bandwidth efficiency versus the number of CM modes for ACM schemes with different SNR ranges

7 Broadband wireless standards for stratospheric communications in millimetre frequency bands

Stratospheric communications are still in their infancy, so no particular standard has yet been specified for the provision of broadband wireless services via stratospheric platforms. Looking at the allocated frequency bands, a terrestrial mobile standard like UMTS in the 2 GHz frequency band is an ideal candidate for providing narrow band mobile services. However, for broadband wireless services only a millimetre frequency band is foreseen. At millimetre frequency bands a line of sight should exist between transmitter and receiver to guarantee a quasi error free telecommunication link. Many terrestrial and satellite standards exist for broadband wireless access (BWA), but only a few of them appear to be appropriate for stratospheric communication systems. The terrestrial standards for BWA are based mainly on orthogonal frequency division modulation (OFDM), for example in fixed WiMAX, or even on the orthogonal frequency division multiple access (OFDMA) link in mobile WiMAX, assuming a frequency selective propagation channel. The main reason for this is the absence of a line of sight between transmitter and receiver. So the received signal is the sum of reflected rays which, due to different delays of the received rays, cause inter-symbol interference and frequency selective propagation channel. The main role of ACM schemes specified in the terrestrial systems is to cope with a frequency selective channel and not with atmospheric impairments which do not emerge in centimetre frequency bands allocated for terrestrial communications. In the perspective of the expected predominately LOS channel conditions, and the application of narrow beam antennas, the stratospheric channel is not expected to be frequency selective, thus the implementation of the OFDM, or even OFDMA, approach would increase the system complexity and consequently the energy consumption, which may cause problems at the stratospheric platforms. So if we limit our selection to single carrier standards with a specified ACM scheme the selection of available standards for downlink transmission is narrowed to:

- the IEEE 802.16 single carrier part of standard [34,35] and
- the digital video broadcasting standard over satellites DVB-S2 [24].S

IEEE standard 802.16 was designed to evolve as a set of air interfaces based on a common MAC protocol, but with physical layer specifications dependent on the spectrum of use and associated regulations. The IEEE standard 802.16 specifies different physical layers for the 2-11 GHz and 10-66 GHz frequency ranges. The 10-66 GHz physical layer assumes line-of-sight propagation with no significant concern over multipath propagation, which is very close to stratospheric propagation conditions. The standard supports adaptive coding and modulation profiles in which modulation (QPSK, 16-QAM, or 64-QAM) and various coding types may be assigned dynamically on a burst-by-burst basis. The most widely used coding types are Type 1, with Reed Solomon codes over GF(256), and Type 2, with concatenated Reed Solomon codes over GF(256), as the outer code, with a block length of 255 bytes, and the block convolutional code (24,16) with puncturing pattern (11,10) as an inner code, resulting in total coding rate of 2/3 for inner codes only. Recommendations suggest symbol rates between 16 and 40 MBauds, which, assuming 64-QAM, translates to data rates as high as 240 Mb/s. A sub-selection of CM modes of IEEE 802.16 standard is listed (Table 3) with SNR switching threshold in dB at a target BER equal to 10^{-4} and calculated spectral efficiency in bits/s/Hz. These results were obtained by computer simulations with SPW simulation tool applying Monte-Carlo simulation approach. The SNR range covered by IEEE CM modes is over 20dB, offering a spectral efficiency from 1.25 bit/s/Hz up to 6.00 bit/s/Hz, which is sufficient to cover impairments caused by heavy rain events. The implementation of the whole set of CM-mode would not necessarily lead to improvement of system performance, because the SNR steps between neighbouring CM modes in the ACM

scheme are small which, assuming an error in SNR estimation, leads to an error of selection of the CM mode.

Mod.	*RS code*	*BCC code*	*SNR [dB]*	*spectral eff.*
QPSK	(255,239)	2/3	4,77	1,25
QPSK	(255,247)	2/3	5,31	1,29
QPSK	(255,251)	2/3	5,98	1,31
QPSK	(255,253)	2/3	6,42	1,32
QPSK	(255,239)	1	9,23	1,87
QPSK	(255,247)	1	9,87	1,94
16QAM	(255,239)	2/3	10,48	2,50
QPSK	(255,251)	1	10,54	1,97
16QAM	(255,247)	2/3	11,12	2,58
QPSK	(255,253)	1	11,18	1,98
QPSK	(255,255)	1	11,81	2,00
16QAM	(255,251)	2/3	11,99	2,62
16QAM	(255,253)	2/3	12,43	2,65
64QAM	(255,239)	2/3	14,94	3,75
64QAM	(255,247)	2/3	15,88	3,87
16QAM	(255,239)	1	15,94	3,75
16QAM	(255,247)	1	16,68	3,87
64QAM	(255,251)	2/3	16,75	3,94
64QAM	(255,253)	2/3	17,39	3,97
16QAM	(255,251)	1	17,45	3,94
16QAM	(255,253)	1	17,99	3,97
16QAM	(255,255)	1	18,92	4,00
64QAM	(255,239)	1	22,00	5,62
64QAM	(255,247)	1	22,64	5,81
64QAM	(255,251)	1	23,31	5,91
64QAM	(255,253)	1	24,25	5,95
64QAM	(255,255)	1	24,78	6,00

Table 3: Performance requirements in AWGN channel for 802.16e system for target BER 10^{-4}

The Digital Video Broadcasting-Satellite (DVB-S2) standard, among others, specifies the physical layer for video broadcasting over satellites [24]. It replaces the outdated standard DVB-S. It is characterized by variable CM modes, which allows different data rates and error protection levels to be used and changed on a frame-by-frame basis. Combined with the use of a return channel this may be used for closed-loop adaptive coding and modulation (ACM), allowing the transmission parameters to be optimized for each individual user and their propagation path conditions. The powerful low density parity check codes (LDPC), concatenated with BCH (Bose-Chaudhuri-Hocquenghem) codes, are used to provide quasi error free transmission for upper protocol layers. The modulation schemes with low pick to average power ratio, namely QPSK, PSK, 16APSK and 32APSK, give the possibility of using an efficient high power amplifier at the transmitter. The set of CM modes specified in DVB-S2 standard covers nearly 20dB of SNR range and spectral efficiency from 0,490 bits/s/Hz to 4.453 bits/s/Hz. DVB-S2 standard does not specify the transmission data rates but, depending on allocated frequency bands, a maximum data rate up to 300 Mbits/s is expected. The set of CM modes and SNR thresholds for a target BER value 10^{-4} is given in Table 4. The BER is estimated by Monte-Carlo simulation with the SPW simulation tool. As was found for IEEE 802.16 standard, the SNR steps between neighbouring CM modes are small, and errors in SNR would make some CM modes avoidable.

Mod.	*LDPC code*	*SNR [dB]*	*spectral eff.*
QPSK	1/4	-2.70	0.490
QPSK	1/3	-1.45	0.656
QPSK	2/5	-0.55	0.789
QPSK	1/2	0.85	0.989
QPSK	3/5	2.05	1.188
QPSK	2/3	2.95	1.322
QPSK	3/4	3.90	1.487
QPSK	4/5	4.53	1.587
QPSK	5/6	5.05	1.655
8PSK	3/5	5.65	1.780
QPSK	8/9	6.06	1.766
QPSK	9/10	6.26	1.789
8PSK	2/3	6.59	1.980
8PSK	3/4	7.86	2.228
16APSK	2/3	8.81	2.637
8PSK	5/6	9.26	2.479
8PSK	8/9	10.05	2.646
8PSK	9/10	10.48	2.679
16APSK	3/4	10.82	2.967
16APSK	4/5	10.92	3.166
16APSK	5/6	11.47	3.300
32APSK	3/4	12.56	3.703
16APSK	8/9	12.72	3.523
16APSK	9/10	12.93	3.567
32APSK	4/5	13.49	3.952
32APSK	5/6	14.07	4.120
32APSK	8/9	15.46	4.398
32APSK	9/10	15.69	4.453

Table 4: Performance requirements in AWGN channel for DVB-S2 system for target BER 10^{-4}

In summary, both DVB-S2 and IEEE 802.16 standards specify sets of CM modes which can cover atmospheric impairments, such as rain attenuation, in stratospheric communication systems. The sum of propagation and processing delays in stratospheric communications is around 25 ms which is much lower than in satellite systems, where a cumulative delay of 300 ms is common. Low propagation delays and slow

variation of channel loss may cause no significant problems [36] in ACM scheme implementation in stratospheric communications. However, the classical SNR estimation, due short training sequences in both standards, may lead to significant decrease of system performance and more sophisticated methods for estimating the channel properties should be applied to increase system performance significantly [38,39].

The return channel is required to transfer channel state information from receiver to transmitter at ACM scheme. Both standards IEEE 802.16 and DVB-S2 by complementary standard for DVB-RCS [33] provide means for implementation of the return channel. In both cases, the return channel is also subject to atmospheric impairment, which may lead to an erroneous return channel and consequently to improper selection of the CM mode at the transmitter. Therefore, for efficient operation of the ACM scheme, additional encoding of information of the CM mode in the return channel is necessary.

8 Conclusion

We have proposed rain fading and tropospheric scintillation models for a stratospheric communication system operating in the millimetre frequency bands. Both models are based on statistical satellite channel models, namely the DLR segment approach for rain attenuation and ONERA approach for scintillation modelling. Parameters of DLR and ONERA models were obtained by statistical processing of measured attenuation in geostationary satellite links. In order to adjust these models to the conditions of stratospheric communications, elevation angle dependency has been introduced, which enables modelling of a stratospheric propagation channel for fixed or mobile communications.

The generated time series that model atmospheric impairment have been applied for testing a heuristic approach of ACM scheme design. The results obtained by computer simulation show that ACM schemes drastically improve the performance in terms of system outage and average system throughput, when designed carefully, i.e. when the SNR range and number of CM modes of the ACM are selected according to the range of channel loss variation.

Two standards which include the specifications for ACM scheme and are suitable for stratospheric communications are proposed, namely the IEEE 802.16 single carrier and ETSI standards for digital video broadcasting over satellites DVB-S2. The CM modes in both standards provide a sufficient range to cover impairment caused by atmosphere in millimetre frequency bands. The system availability may be increased by applying new methods for increasing communication link reliability or capacity, such as the multiple input multiple output (MIMO) approach, which has proved to be very efficient in terrestrial systems. The approach of the transmit antennas selection [40,41] in order to maximize system throughput is very powerful, promising the application of linear detection and keeping the system performance close to the performance of optimum detection. These approaches are not directly applicable to stratospheric communications because of a predominately line of sight channel. However, by introducing the concept of distributed MIMO in stratospheric communications, where all platforms transmit the same information, but not necessarily the same symbols, further increase of system performance is expected. Communication between platforms is essential in the distributed MIMO approach in order to spread information among platforms and for collaborative signal detection, so that reliable inter-platform links are required, similar to those in satellite systems [42].

Acknowledgment:

This work has been partially funded by the European Community through the 6th Framework Programme IST project SatNEx (FP6-IST-027393).

References:

[1] E. Lutz, M. Werner, A. Jahn, *Satellite Systems,* Springer-Verlag, 2000.

[2] G. Maral, M. Bosquet, *Satellite Communications Systems*, Second Edition, John Willey & Sons, 1993.

[3] W. T. Webb, L. Hanzo, *Modern Quadrature Amplitude Modulation*, Pentech Press Ltd, London, 1994.

[4] A. J. Goldsmith and S. G. Chua, Adaptive coded modulation for fading channels, *IEEE Trans. Commun.*, Vol. 46, No. 5, 1998, pp. 595-602.

[5] K. J. Hole, H. Holm, G. E. Oien, Adaptive coded modulation performance and channel estimation tools for flat fading channels, *IEEE J. Selec. Areas Commun.*, Vol. 18, No. 7, 2000, pp. 1153-1158.

[6] J. Williams, L. Hanzo and R. Steele, Channel-adaptive modulation, *6th IEE International Conference on Radio Receivers and Associated Systems*, London, 1999, pp. 144-147.

[7] T. Javornik, G. Kandus, An Adaptive Rate Communication System Based on the N-MSK Modulation Technique, *IEICE Trans. Commun.,* Vol. E84-B, No. 11, 2001, pp. 2946-2955.

[8] U. Toyoki, S. Sampei, N. Morinaga, K. Hamaguchi, Symbol Rate and Modulation Level-Controlled Adaptive Modulation/TDMA/TDD System for High-Bit-Rate Wireless Data Transmission, *IEEE Trans. on Vehicular Technology.* Vol. 47, No. 4, 1998, pp. 1134-1147.

[9] G. Kandus, Broadband Communications from High Altitude Platforms, Plenary Lecture, *WSEAS International Conference on Circuits, Systems, Signals and Telecommunications (CISST'07),* Jan. 17-19. 2007, Queensland, Australia.

[10] G.M. Djuknic, J. Freidenfelds, and Y. Okunev, Establishing Wireless Communications Services via High-Altitude Aeronautical Platforms: A Concept Whose Time Has Come? *IEEE Commun. Mag.,* Vol. 35, No. 9, Sept. 1997, pp. 128-35.

[11] M. Mohorcic, D. Grace, G. Kandus, T. Tozer, Broadband Communications from Aerial Platform Networks, *In: Proc. of the 13th IST Mobile and Wireless Communications Summit 2004,* Lyon, France, June 27-30, 2004, pp. 257-261.

[12] D. Grace, M. H. Capstick, M. Mohorcic, J. Horwath, M. Bobbio Pallavicini, M. Fitch, Integrating Users into the Wider Broadband Network via High Altitude Platforms, *IEEE Wireless Communications*, Vol. 12, No. 5, 2005, pp. 98-105.

[13] T. C. Tozer and D. Grace, High-Altitude Platforms for Wireless Communications, *Electronics & Communication Engineering Journal*, Vol. 13, No. 3, 2001, pp. 127-137.

[14] T. Javornik, M. Mohorčič, A. Švigelj, I. Ozimek and G. Kandus, Adaptive coding and modulation for mobile wireless access via high altitude platforms, *Wireless Personal Communications*, Vol. 32, No. 3-4, 2005, pp. 301-17.

[15] S. Plevel, T. Javornik, M. Mohorčič and G. Kandus, Empirical Propagation Channel Model for High Altitude Platform Communication Systems, in *Proc. 11th Ka and Broadband Communications Conference*, Rome, Italy, 25-28 Sept. 2005.

[16] G. Kandus, M. Mohorčič, E. Leitgeb, T. Javornik, Modelling of Atmospheric Impairments in Stratospheric Communications, *2nd WSEAS International Conference on Circuits, Systems, Signal and Telecommunications (CISST'08),* Acapulco, Mexico, January 25-27, 2008.

[17] U.-C. Fiebig, L. Castanet, J. Lemorton, E. Matricciani, F. Pérez-Fontán, C. Riva and R. Watson, Review of Propagation Channel Modelling, in *Proc. 2nd Workshop of the COST 272-280 Action "Propagation Impairment Mitigation for Millimetre Wave Radio Systems",* Noordwijk, Holland. May 2003.

[18] L. Castanet, T. Deloues and J. Lemorton, Methodology to Simulate Long-term Propagation Time-series from the Identification of Attenuation Periods Filled with Synthesized Events, in *Proc. 2nd Workshop of the COST 272-280 Action "Propagation Impairment Mitigation for Millimetre Wave Radio Systems",* Noordwijk, Holland, May 2003.

[19] U.-C. Fiebig, A Time-Series Generator Modelling Rain Fading, in *Proc. Proc. Open Symposium on Propagation and Remote Sensing, URSI Commission F,* Espoo Finland, Oct. 2002.

[20] European Centre for Medium-Range Weather Forecasts, http://www.ecmwf.int

[21] Attenuation by hydrometers, in precipitation, and other atmospheric particles, CCIR Report 721-1, Propagation in Non-Ionized Media, CCIR, Geneva, 1980.

[22] ITU-R P Radiowave propagation (P-series) of recommendations, 2002

[23] ITU-R Recommendation, PN 618-3: Propagation data and prediction methods required for the design of earth-space telecommunication systems, ITU, 1994

[24] ETSI EN 302 307 (V1.1.2), Digital Video Broadcasting (DVB): Second generation framing structure, channel coding and modulation systems for Broadcasting, interactive Services, News gathering and other broadband satellite applications," European Telecommunications Standards Institute (ETSI), June 2006.

[25] P. Yu, I. A. Glover, P. A. Watson, O. T. Davies, S. Ventouras and C. Wrench, Review and Comparison of Tropospheric Scintillation Prediction Models for Satellite

Communications, *International Journal of Satellite Communications and Networking*, Vol. 24, Issue 4, 2006, pp. 261-317.

[26] E. Matricciani, M. Mauri and C. Riva, Relationship between Scintillation and Rain Attenuation at 19.77 GHz, *Radio Science*, Vol. 31, No. 2, 1996, pp. 273-279.

[27] F. Lacoste, J. P. Millerioux, L. Castanet and C. Riva, Generation of Time Series of Scintillation Combined with Rain Attenuation, in *Proc. ECPS 2005 Conference,* Brest, France, March 2005.

[28] C. Spillard, E. Falletti, J. D. Penin, J. L. Ruíz-Cuevas and M. Mondin, *Mobile Link Propagation Aspects, Channel Model and Impairment Mitigation Techniques*, FP6 IST-2003-506745 CAPANINA, Deliverable D14, 2004.

[29] V. I. Tatarskii, *Wave Propagation in a Turbulent Media*, McGraw-Hill, New York, U.S.A., 1961.

[29] D. Vanhoenacker-Janvier and H. Vasseur, Prediction of Scintillation Effects on Satellite Communications above 10 Ghz, *IEE Proceedings-Microwaves, Antennas and Propagation*, Vol. 142, No. 2, 1995, pp. 102-8.

[30] G. Albertazzi et al., On the Adaptive DVB-S2 Physical Layer: Design and performance, *IEEE Wireless Communications*, Vol. 12, No. 6, December 2005, pp. 62-68.

[31] A. Morello and V. Mignone, DVB-S2: The second Generation Standard for Satellite Broad-band Services, *Proceedings of the IEEE*, Vol. 94, No. 1, January 2006, pp. 210-227.

[32] ETSI EN 300 421 (V.1.1.2): Digital Video Broadcasting (DVB); Framing structure, channel coding and modulation for 11/12 GHz satellite services.

[33] ETSI EN 301 790: Digital Video Broadcasting (DVB); Interaction channel for satellite distribution systems

[34] IEEE 802.16-2004, IEEE Standard for Local and metropolitan area networks Part 16: Air Interface for Fixed Broadband Wireless Access Systems, IEEE, October 1, 2004.

[35] T. Cooklev, *Wireless Communication Standards; A Study of IEEE 802.11, 802.15 and 802.16,* IEEE Standard Wireless Networks Series, IEEE Press 2004.

[36] M. Smolnikar, T. Javornik, M. Berioli and M. Mohorcic, DVB-S2 Adaptive Coding and Modulation for HAP Communication System, *in Proceeding of the 67th IEEE Vehicular Technology Conference (VTC2008-Spring)*, Marina bay, Singapore, May 2008.

[38] M. Smolnikar, T. Javornik and M. Mohorčič, Channel decoder assisted adaptive coding and modulation for HAP communications, *in Proceeding of the 65th IEEE Vehicular Technology Conference (VTC2007-Spring),* Dublin, Ireland, April 2007.

[39] M. Smolnikar, M. Mohorčič and T. Javornik, Utilisation of LDPC decoder parameters in DVB-S2 ACM procedures, *in Proceeding of the International Workshop on Satellite and Space Communication (IWSSC'07),* Salzburg, Austria, September 2007.

[40] G. Kandus, S. Plevel, T. Javornik, Advanced V-BLAST detection algorithm in multi-model spatial multiplexing MIMO systems, WSEAS Trans. Commun., Vol. 5, No. 2, 2006, pp 202-209.

[41] S. Plevel, T.Javornik, G. Kandus, I. Jelovčan, Transmission Scheme Selection Algorithm for spatial multiplexing MIMO systems with linear detection, WSEAS Trans. Commun., Vol. 5, No. 6, 2006, pp. 1169-1176.

[42] A. Švigelj, M. Mohorčič, G. Kandus, Adaptive packet routing on traffic class differentiation in intersatellite link networks, WSEAS Trans. Commun., Vol. 1, No. 1, 2002, pp. 138-143